Comparative Spectroscopic and Reactivity Studies of $Sc_{3-x}Y_xN@C_{80}$ ($x = 0-3$)

Ning Chen,[†] Lou-Zhen Fan,[‡] Kai Tan,[§] Yue-Qin Wu,[‡] Chun-Ying Shu,[†] Xin Lu,*[,§] and Chun-Ru Wang*[,†]

Beijing National Laboratory for Molecular Sciences, Institute of Chemistry, Beijing 100080, China, State Key Laboratory of Physical Chemistry of Solid Surface, Center for Theoretical Chemistry, Departmental of Chemistry, Xiamen University, Xiamen 361005,China, and Department of Chemistry, Beijing Normal University, Beijing 100000, China.

Received: April 26, 2007; In Final Form: May 24, 2007

A series of endohedral fullerenes $Sc_{3-x}Y_xN@C_{80}$ ($x = 0-3$) with variable encaged moieties and the same C_{80} cage were synthesized, isolated, and spectroscopically characterized by the laser desorption time-of-flight mass spectrometry (LD-TOF−MS), differential pulse voltammetry (DPV), Fourier transform infrared (FTIR), visible-near-infrared (vis-NIR) absorption spectrometry, and so forth. It was revealed that $Sc_{3-x}Y_xN@C_{80}$ ($x = 0-3$) have a similar electronic structure, $(Sc_{3-x}Y_xN)^{6+}@(C_{80})^{6-}$. However, because of the relatively larger van der Waals radius of yttrium to that of scandium which induces the size increase of $Sc_{3-x}Y_xN$ from $x = 0$ to $x = 3$, the frontier orbitals of this series of endohedral fullerenes dramatically change. For example, $Sc_2YN@C_{80}$ shows similar electronic property with its left neighbor $Sc_3N@C_{80}$ but is quite different with its right neighbor $ScY_2N@C_{80}$. The cycloaddition reactions of *N*-enthylazomethine ylide with $Sc_{3-x}Y_xN@C_{80}$ ($x = 0-3$) were carried out, and the regioselectivity of endohedral fullerenes shows the same trend of variation to that of their electronic properties along with the size of endohedral moiety increasing. It was found that $Sc_3N@C_{80}$ and $Sc_2YN@C_{80}$ produce only the [5,6]-pyrrolidine regioisomers, and a critical change in fullerene regioselectivity occurs from $ScY_2N@C_{80}$ where the [6,6]-pyrrolidine regioisomer appears as a minor regioisomer and finally becomes the major regioisomer in the case of $Y_3N@C_{80}$.

Introduction

Endohedral fullerenes, featuring as fullerenes encapsulating one or several atoms, ions, or atomic clusters, are highly interesting because of their novel properties[1] and potential applications[2] in electronics, optics, biology, medicine, nanomaterials, and so forth. Up-to-date scientists have synthesized, isolated, and spectroscopically characterized hundreds of endohedral fullerenes, with the parent fullerene cages varying from C_{60} to C_{100}, and the encaged species covering hydrogen,[3] nitrogen,[4] noble gases,[5] alkaline earth metals,[6] transition metals,[7] lanthanide metals,[8] and even atomic clusters such as metal carbides[9] and metal nitrides.[10]

Endohedral fullerenes are usually accompanied with electron transfers from the endohedral moieties to carbon cages;[1] that is, the molecular electronic structure can be described as $En^{m+}@C_{2n}^{m-}$. Because the entrapment of endohedral moieties within fullerene cages prevents it from an exoteric chemical attack, it is generally believed that the reactivity of endohedral fullerenes is dominated by the fullerene cages, and several early experiments showed a similar reactivity of $M@C_{82}$ (M = Y, La, Ce, Pr) that seemingly supported this supposition.[11] Recently, however, a comparative study[13] for $(La_2)^{6+}@C_{80}^{6-}$ and $(Sc_3N)^{6+}@C_{80}^{6-}$ revealed their obviously different reactivity; that is, $Sc_3N@C_{80}$ has much lower thermal reactivity toward disilirane than $La_2@C_{80}$, though both of them share the fullerene cage I_h-C_{80}^{6-}. Another study of $Sc_3N@C_{80}$ and $Y_3N@C_{80}$[14a] further revealed different regioselectivities of metallofullerenes with different endohedral moieties: the 1,3-dipolar cycloaddition (1,3-DC) reactions were observed to occur at a [5,6] ring junction of $Sc_3N@C_{80}$ but at a [6,6] ring junction of $Y_3N@C_{80}$.

For revealing how the size of encaged moiety of endohedral fullerenes affects their chemical reactions, we recently synthesized a series of endohedral fullerenes, that is, $Sc_{3-x}Gd_xN@C_{80}$ ($x = 0-3$), and made a systematic study on their reactivities.[15] The results show clearly that along with the size of $Sc_{3-x}Gd_xN$ increasing, the fullerene regioselectivity gradually changes from [5,6]-cycloaddition to [6,6]-cycloaddition. However, this study did not relate the reactivity of $Sc_{3-x}Gd_xN@C_{80}$ ($x = 0-3$) to their electronic properties, because on the one hand, the low yield of Gd-based fullerenes makes it difficult to characterize their electronic properties and, on the other hand, the super paramagnetic property of Gd-based fullerenes prohibit them from the important NMR characterization of the reacting products.

Here, we alternatively synthesized a series of endohedral fullerenes $Sc_{3-x}Y_xN@C_{80}$ ($x = 0-3$) and made a detailed comparative study on their electronic property and reactivity. Because of the relative large amount of $Sc_{3-x}Y_xN@C_{80}$ samples, it is possible to fully characterize the endohedral fullerenes via various spectrometries such as the laser desorption time-of-flight mass spectrometry (LD-TOF−MS), differential pulse voltammetry (DPV), Fourier transform infrared (FTIR), visible-near-infrared (vis-NIR) absorption spectrometry, and so forth. These studies revealed their electronic properties clearly. The cycloaddition of these endohedral fullerenes were also studied, and

* Corresponding authors. Phone and Fax: (+86)10-62652120, e-mail: crwang@iccas.ac.cn (C.-R.W.). Phone and Fax: (+86)10-62568158, e-mail: xinlu@xmu.edu.cn (X.L.).
[†] Institute of Chemistry.
[‡] Xiamen University.
[§] Beijing Normal University.

10.1021/jp073229a CCC: $37.00
Published on Web 07/19/2007

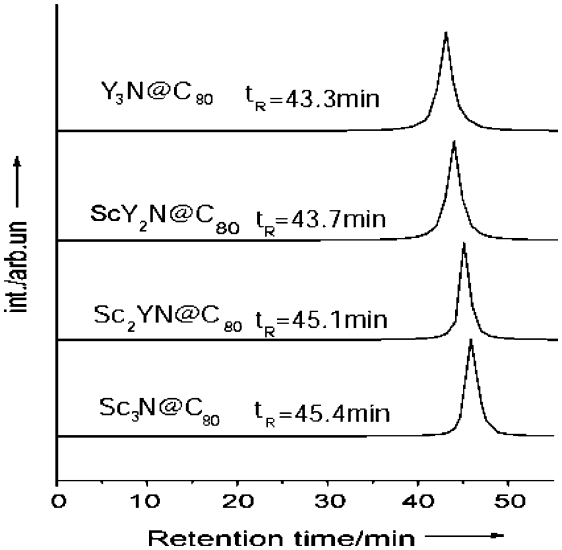

Figure 1. Chromatograms of the isolated $Sc_{3-x}Y_xN@C_{80}$ ($x = 0-3$) shows different retention times for them in Buckyprep column (toluene eluent at 12 mL/min).

the reaction products were also well characterized by HPLC, LD-TOF MS, and ^1H and ^{13}C NMR spectrometry.

Furthermore, on the basis of the above experimental investigations, we have also performed ab initio calculations on the electronic structures and reactivity of these endohedral fullerenes. The combined experimental and theoretical studies allow us not only to observe how the electronic properties of $Sc_{3-x}Y_xN@C_{80}$ change with the size of the encaged moieties but also to relate the fullerene electronic properties to their reactivity directly.

Experimental Section

Fullerene soot is produced by arc-burning Sc/Y/graphite composite rods (atomic ratio of Sc:Y:C is ca. 1:1:24) under an atmosphere of He (99%)/N_2(1%) mixture at 300 Torr. The soot was collected in ambient condition and Soxhlet-extracted with toluene for 20 h. Soot extracts contain both empty fullerenes such as C_{60} and C_{70} and endohedral fullerenes such as $Sc_2@C_{2n}$ ($2n = 70-90$), $Sc_{3-x}Y_xN@C_{80}$ ($x = 0-3$). Multistage HPLC technique is employed to isolate and purify the endohedral fullerenes, using two complementary columns: Cosmosil Buckyprep and Cosmosil Buckyprep-M. To ascertain a high purity of the samples, each isolated $Sc_{3-x}Y_xN@C_{80}$ ($x = 0-3$) is confirmed to have a single-peak HPLC profile (Figure 1) and a single-peak in both negative ionic and positive ionic mass spectra of corresponding samples (Figure S3, Supporting Information).

For the fullerene reactions, approximately 2.0 mg of purified (99%) metallofullerenes ($Sc_3N@C_{80}$, $Sc_2YN@C_{80}$, $ScY_2N@C_{80}$, and $Y_3N@C_{80}$) are dissolved in 10 mL of *o*-dichlorobenzene solutions and heated to 115 °C; then, an excess of *N*-enthyl glycine (25 fold) and ^{13}C-enriched paraformaldehyde (125 fold) were added to them separately under argon atmosphere. The reaction products are purified by HPLC with a Cosmosil Buckyprep-M column (Φ 20 × 250 mm, toluene eluent, flow rate of 12 mL/min).

Results and Discussion

Synthesis and Isolation of the $Sc_{3-x}Y_xN@C_{80}$ ($x = 0-3$). Endohedral fullerenes $Sc_{3-x}Y_xN@C_{80}$ ($x = 0-3$) are prepared by the Krätschmer−Huffman method and isolated by multistage HPLC technique. $Sc_3N@C_{80}$ were isolated from the soot extract (Sc/C composite rods arc-discharge) and purified via a two-stage high-performance liquid chromatography (HPLC) process. Buckyprep column separates fullerenes according to their size. In the first stage, the Buckyprep column was used to collect the $C_{88}-C_{90}$ fraction. The Buckyprep-M column, which separates fullerenes according to their polarity, was employed in the second stage to remove the hollow fullerenes (C_{88}, C_{90}) from $Sc_3N@C_{80}$. Stages 1 and 2 were repeated several times until pure $Sc_3N@C_{80}$ was being collected. $Y_3N@C_{80}$ was separated via a similar process (soot extract from Y/C composite rods arc-discharge) as $Sc_3N@C_{80}$; only the collection fractions are different for them because of the different retention times of $Sc_3N@C_{80}$ and $Y_3N@C_{80}$.

$Sc_2YN@C_{80}$ and $ScY_2N@C_{80}$ were isolated from the soot extract (Sc/Y/C composite rods arc-discharge) and purified via a four-stage HPLC process. The first stage of HPLC utilized the Buckyprep column to collect the $C_{88}-C_{90}$ fraction; the second stage was performed in a Buckyprep-M column to remove the hollow fullerenes. The third stage of HPLC utilized the Buckyprep column again, but a recycling function is employed to separate $Sc_3N@C_{80}$, $Sc_2YN@C_{80}$, $ScY_2N@C_{80}$, and $Y_3N@C_{80}$ into four different fractions. The fourth stage HPLC used the Buckyprep column in recycling mode to purify the isolated $Sc_2YN@C_{80}$ and $ScY_2N@C_{80}$.

Figure 1 shows that $Sc_2YN@C_{80}$ and $ScY_2N@C_{80}$ have almost the same retention time with $Sc_3N@C_{80}$ and $Y_3N@C_{80}$ off the Buckyprep column respectively, suggesting that $Sc_2YN@C_{80}$ and $Sc_3N@C_{80}$ have similar size and polarity. Moreover, $Sc_2YN@C_{80}$ and $ScY_2N@C_{80}$ have almost the same retention time on Buckyprep-M and Buckyclutcher columns while their retention time on Buckyprep column is similar but different, indicating that they may have similar polarities.

Spectroscopic Study of $Sc_xY_{3-x}N@C_{80}$ ($x = 0-3$). UV−vis-NIR spectra of $Sc_{3-x}Y_xN@C_{80}$ ($x = 0-3$) are measured and shown in Figure 2a. The strongest absorption for $Sc_3N@C_{80}$, $Sc_2YN@C_{80}$, $ScY_2N@C_{80}$, and $Y_3N@C_{80}$ are 385, 378, 430, and 409 nm, respectively. The electronic absorption spectra of four $Sc_{3-x}Y_xN@C_{80}$ ($x = 0-3$) endohedral fullerenes are similar to each other. Electronic absorptions of endohedral fullerenes mainly depend on the structure and charge state of the carbon cage. It is known that both $Sc_3N@C_{80}$ and $Y_3N@C_{80}$ share the same C_{80}-I_h fullerene cage and the M_3N (M = Sc, Y) donate six electrons to the C_{80} cage;[16] so, the overall resembling absorption spectra of the $Sc_{3-x}Y_xN@C_{80}$ ($x = 0-3$) suggest that these fullerenes have a similar electronic structure, that is, $(Sc_{3-x}Y_xN)^{6+}@C_{80}^{6-}$. Figure 1b shows selected range of the FTIR spectra of the four samples. They have similar fingerprint peaks of C_{80}^{6-} at approximately 1200 and 1380 cm^{-1} which further supports above assignments. In fact, so far, all of the isolated $M_3N@C_{80}$ endohedral fullerenes[17] such as $Gd_3N@C_{80}$, $Dy_3N@C_{80}$, $Tm_3N@C_{80}$, $ScYErN@C_{80}$, and $Sc_2ErN@C_{80}$ were reported to have similar geometric structures as well as electronic structures. On the other hand, in the region of 600−800 cm^{-1}, which are assigned as the antisymmetric M−N stretching vibration because of the metal dependence,[18] a significant difference was observed for $Sc_{3-x}Y_xN@C_{80}$ ($x = 0-3$). In particular, while a strong absorption was observed in $Sc_3N@C_{80}$ (599 cm^{-1}) and a small absorption split for $Y_3N@C_{80}$ (726 cm^{-1}, 714 cm^{-1}) as previously reported,[18] IR absorption split into two parts for $Sc_2YN@C_{80}$ (676 cm^{-1}, 647 cm^{-1}) and $ScY_2N@C_{80}$(736 cm^{-1}, 699 cm^{-1}). The increasing split hints to an increasing distortion of trigonal geometry. These results are similar to those of previous reported $Sc_{3-x}Gd_xN@C_{80}$ ($x = 0-3$)[12] and $Sc_{3-x}Er_xN@C_{80}$ ($x = 0-3$).[18]

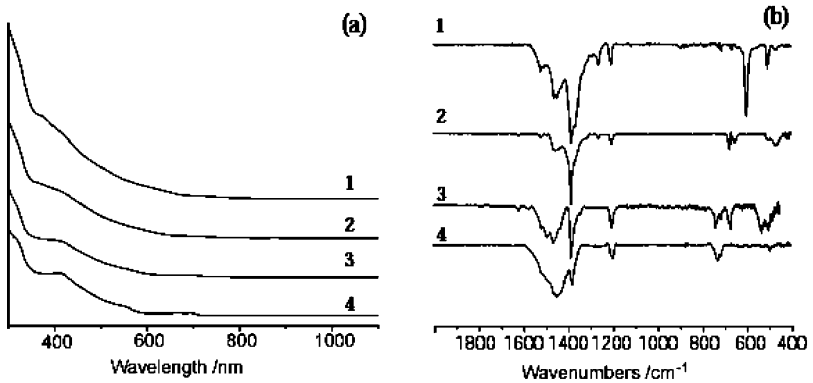

Figure 2. Spectroscopic characterizations of $Sc_{3-x}Y_xN@C_{80}$($x = 0-3$). (a) UV−vis-NIR spectra, (b) FTIR spectra. 1:$Sc_3N@C_{80}$, 2:$Sc_2YN@C_{80}$, 3:$ScY_2N@C_{80}$, 4:$Y_3N@C_{80}$.

C_{80}-I_h has fourfold degenerate highest occupied molecular orbitals (HOMOs) with only two electrons occupied; so, the C_{80} moiety in $M_3N@C_{80}$ can receive 6 electrons from the M_3N moiety to form a stable closed-shell electronic structure, $(Sc_{3-x}Y_xN)^{6+}@C_{80}^{6-}$. As a result, the HOMOs of $M_3N@C_{80}$ are mainly localized on the C_{80}^{6-}, whereas the lowest unoccupied molecular orbitals (LUMOs) are contributed by both C_{80}^{6-} and M_3N^{6+}.[13] As such, the difference in the electronic properties of $M_3N@C_{80}$ with different M_3N mieties, if any, should be dominated by the nature of their LUMOs, that is, different composition of the LUMOs from the orbitals of the C_{80} and M_3N fragments. Indeed, $Sc_3N@C_{80}$ and $Y_3N@C_{80}$ were revealed to have a different reactivity in the regioselectivity of C_{80} cages;[14a] therefore, some differences in their molecular LUMOs are expected. A comparative study of $Sc_{3-x}Y_xN@C_{80}$ ($x = 0-3$) will be helpful to distinguish the differences and make clear where the difference originates.

Though the main features of UV−vis-NIR spectra (Figure 2a) of $Sc_{3-x}Y_xN@C_{80}$ ($x = 0-3$) are similar, if we focus on the optical onsets and nearby absorption peaks that correspond to the electronic transitions involving HOMOs and/or LUMOs, surprisingly then, remarkable differences can be found between them. The HOMO−LUMO transition of $ScY_2N@C_{80}$ has a doublet structure with absorption maxima at 665 and 693 nm. These features are quite similar to those of $Y_3N@C_{80}$ which show HOMO−LUMO transitions with absorption maxima at 664 and 693 nm. However, $Sc_2YN@C_{80}$ exhibits singlet HOMO−LUMO transitions at 723 nm which resembles that of $Sc_3N@C_{80}$ (735 nm). Thus, the four $Sc_{3-x}Y_xN@C_{80}$ ($x = 0-3$) members can be classified into two groups, in which $Sc_3N@C_{80}$ and $Sc_2YN@C_{80}$ showing close resemblances on both absorption on-set and nearby absorption peaks in the spectra are named as group 1 and $ScY_2N@C_{80}$ and $Y_3N@C_{80}$ are similarly named as group 2 (Figure 3). A critical change occurs at the point from $Sc_2YN@C_{80}$ to $ScY_2N@C_{80}$. This result completely agrees with that of recently reported $Sc_{3-x}Gd_xN@C_{80}$ ($x = 0-3$).[12]

On the basis of the spectral onsets, their optical energy gaps were calculated. In spite of the obvious difference between these two groups, their optical energy gaps are quite close, which range from 1.50 eV for $Sc_3N@C_{80}$ to 1.71 eV for $Y_3N@C_{80}$. Since an energy gap value of 1.0 eV marks the borderline between large and low-energy gap fullerenes, these four TNT fullerenes are classified as large energy gap fullerenes.

Electrochemistry Study of $Sc_{3-x}Y_xN@C_{80}$ ($x = 0-3$). To get more details of the electronic structures and chemical properties of these fullerenes, cyclic voltammograms (CVs) and the differential pulse voltammograms (DPV) of $Sc_{3-x}Y_xN@C_{80}$ ($x = 0-3$) in *o*-dichlorobenzene were studied, and they all show

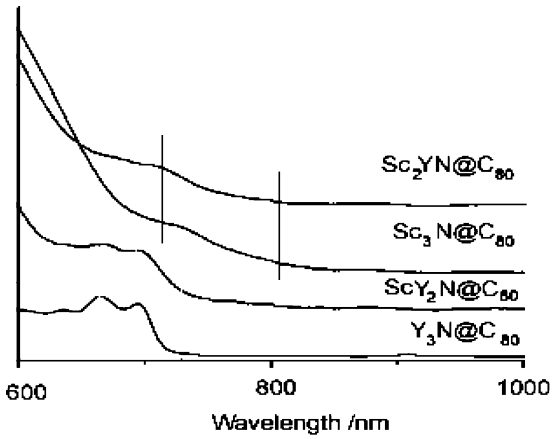

Figure 3. On-sets and nearby absorption peaks in UV−vis-NIR absorption spectra of $Sc_{3-x}Y_xN@C_{80}$ ($x = 0-3$).

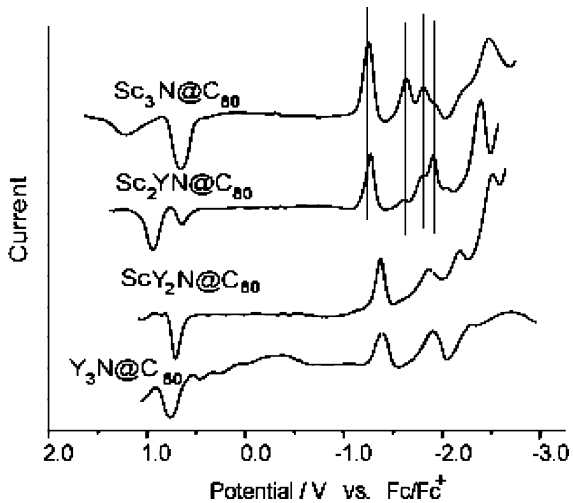

Figure 4. DPVs of $Sc_{3-x}Y_xN@C_{80}$ ($x = 0-3$) in *o*-dichlorobenzene containing 0.1 M TBAPF6 at a 50 mV/s scan rate, 50 mV pulse, 50 ms pulse width, and 200 ms period.

similar features for the four members of this endohedral fullerene family, suggesting similar electronic structures of this series of endohedral fullerenes. However, both CV and DPV of $Sc_{3-x}Y_xN@C_{80}$ ($x = 0-3$) are far from identical, reflecting their subtle differences in molecular frontier orbitals. Figure 4 shows the DPV of $Sc_{3-x}Y_xN@C_{80}$ ($x = 0-3$) in *o*-dichlorobenzene. Obviously, the DPV patterns of $Sc_2YN@C_{80}$ and $Sc_3N@C_{80}$ are essentially the same while those of $ScY_2N@C_{80}$ and $Y_3N@C_{80}$ are also; the main differences were observed to occur beginning from $Sc_2YN@C_{80}$ to $ScY_2N@C_{80}$. Moreover, the

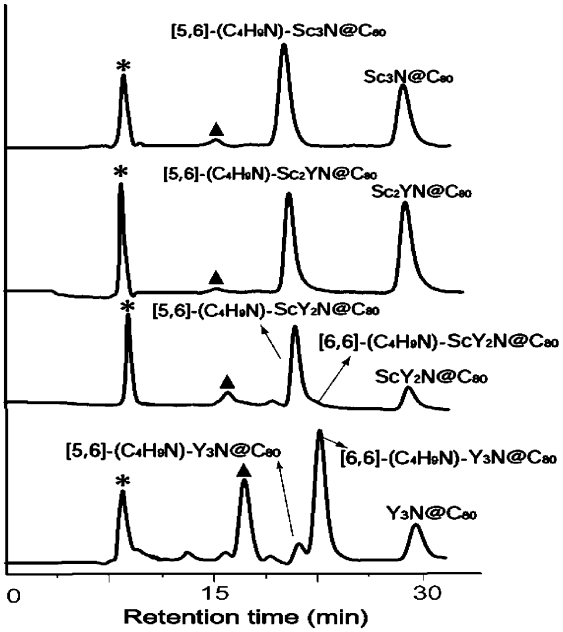

Figure 5. HPLC (Buckyprep-M, toluene eluent at 12 mL/min) profile of the reacting products in the 1,3-dipolar cycloaddition reaction of *N*-enthylazomethine ylide, in which pyrrolidinofullerenes $[C_4H_9N]$-$Sc_{3-x}Y_xN@C_{80}$ ($x = 0-3$) are the main products; (*) denotes *o*-dichlorobenzene peak and (▲) denotes bisadducts of $Sc_{3-x}Y_xN@C_{80}$ ($x = 0-3$) fullerenes.

electrochemical gaps of $Sc_{3-x}Y_xN@C_{80}$ ($x = 0-3$) result from the potential difference between their first reduction and their first oxidation steps which are 1.91, 1.94, 2.07, and 2.15 V, respectively, consistent with the order of optical energy gaps obtained from UV-vis-NIR absorption spectrometry.

Chemical Reactivity Study of $Sc_{3-x}Y_xN@C_{80}$ ($x = 0-3$). Since $Sc_{3-x}Y_xN@C_{80}$ ($x = 0-3$) show different electronic properties, they must sometimes display different chemical reactivity too. In fact, different regioselectivities for $Sc_3N@C_{80}$ and $Y_3N@C_{80}$ were just reported.[14] Now that group 1 and group 2 metallofullerenes separately show similar in-group electronic properties and obvious differences between groups, we may reasonably presume that $Sc_{3-x}Y_xN@C_{80}$ ($x = 0-3$) have their regioselectivities changing at the point from $Sc_2YN@C_{80}$ to $ScY_2N@C_{80}$ in reactivity. Therefore, we performed a comparative study on the $Sc_{3-x}Y_xN@C_{80}$ ($x = 0-3$) chemical reactions by following a standard procedure of the 1,3-dipolar cycloaddition reaction of *N*-enthylazomethine ylide.[14,19-23]

In our experiments, first, four metallofullerene solutions ($Sc_3N@C_{80}$, $Sc_2YN@C_{80}$, $ScY_2N@C_{80}$ and $Y_3N@C_{80}$ in *o*-dichlorobenzene) were heated to 115 °C; afterward, ^{13}C enriched formaldehyde and an excess of *N*-ethyl glycine were added to react with the metallofullerenes under the same temperature. The experimental conditions for the four samples were carefully kept identical for comparison. After 15 min reaction time, the samples were cooled and HPLC with a Buckyprep-M column was applied to isolate the reacting products. The resulting HPLC profiles for the four samples were shown in Figure 5. Each fraction of the HPLC profiles was collected and analyzed by MALDI-MS to determine the composition, in which the fractions with retention time at 19.6−23.9 min were assigned as the pyrrolidinofullerene monoadducts (Figure S4, Supporting Information), and other fractions were o-dichlorobenzene, the unreacted $Sc_{3-x}Y_xN@C_{80}$, and pyrrolidinofullerene biadducts, respectively.

Because the cycloaddition reactions of *N*-enthylazomethine ylide with $Sc_3N@C_{80}$ and $Y_3N@C_{80}$ under similar conditions have been studied previously,[14,19-24] the monoaddition derivative of $Sc_3N@C_{80}$ was known to be the [5,6]-$[C_4H_9N]$-$Sc_3N@C_{80}$ regioisomer,[14a] and that of $Y_3N@C_{80}$ was the [6,6] regioisomer. As shown in Figure 4, the [5,6]-$[C_4H_9N]$-$Sc_3N@C_{80}$ and [6,6]-$[C_4H_9N]$-$Y_3N@C_{80}$ have different retention times at 20.1 and 22.7 min, respectively, and the *N*-ethyl pyrrolidino-$Y_3N@C_{80}$ has a minor regioisomer appear before [6,6]-$[C_4H_9N]$-$Y_3N@C_{80}$ which was assigned as the [5,6]-$[C_4H_9N]$-$Y_3N@C_{80}$.[22a] The composition of this fraction was determined by MALDI-MS to be $[C_4H_9N]$-$Y_3N@C_{80}$, and after the heat treatment of the sample at 180 °C for 1 h, the peak for this fraction increases largely, indicating that most [6,6]-$[C_4H_9N]$-$Y_3N@C_{80}$ was converted to [5,6] regioisomer. It shows that the [6,6] addition is kinetically controlled, but the [5.6] adduct is thermodynamically more stable. This phenomena was also reported by Echegoyen et al.[22] Obviously, the retention times of the *N*-ethyl pyrrolidinofullerenes depend mainly on the [5,6] or [6,6] regioisomers but not on the metallofullerene ($Sc_xY_{3-x}N@C_{80}$) composition, and then may be used as a convenient criterion to distinguish different regioisomers of the $M_3N@C_{80}$ analogues.

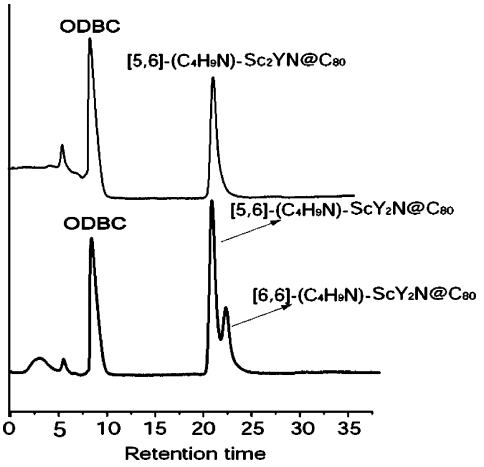

Figure 6. Comparative study of the HPLC (Buckyprep-M, toluene, 12 mL/min) profiles of [5,6]-pyrrolidino−$Sc_2YN@C_{80}$ and [5,6]/[6,6]-pyrrolidino−$ScY_2N@C_{80}$.

In Figure 5, it was observed that the monoaddition pyrrolidino-$Sc_3N@C_{80}$, -$Sc_2YN@C_{80}$, and -$ScY_2N@C_{80}$ nearly have the same retention times, so the derivatives of $Sc_2YN@C_{80}$ and $ScY_2N@C_{80}$ are also the [5,6] regioisomers similar to the [5,6]-$[C_4H_9N]$-$Sc_3N@C_{80}$. However, the [5,6]-$[C_4H_9N]$-$ScY_2N@C_{80}$ peak has a broad tail in the HPLC profile, suggesting the presence of the minor [6,6]-pyrrolidino-$ScY_2N@C_{80}$ regioisomer. We collected the pyrrolidinofullerene fractions of $Sc_2YN@C_{80}$ and $ScY_2N@C_{80}$ with retention times at 21.4−23.9 min, and we performed the HPLC again. It can be seen that the former sample maintains a single peak while the latter sample shows two distinct peaks (Figure 6) in the HPLC profiles. Obviously, the new peak corresponds to [6,6]-$[C_4H_9N]$-$ScY_2N@C_{80}$ because of its similar retention time (22.4 min) to [6,6]-$[C_4H_9N]$-$Y_3N@C_{80}$. It was estimated that the molar ratio of [6,6] to [5,6] regioisomers of $C_4H_9N-ScY_2N@C_{80}$ is 1:47 from the HPLC chromatography.

The above regioisomer assignment based on the HPLC retention times was further confirmed by NMR spectrometry studies on the purified $C_4H_9N-Sc_2YN@C_{80}$ and the major isomer of $C_4H_9N-ScY_2N@C_{80}$. Both of their ^{13}C NMR spectra (Figure 7) exhibit an identical single-peak at 69.95 ppm, which is consistent with the single NMR line (70.09 ppm) of the [5,6]-pyrrolidino-$Sc_3N@C_{80}$ derivative but is different from the two NMR line patterns of the [6,6]-pyrrolidino-$Y_3N@C_{80}$ derivative.[14a]

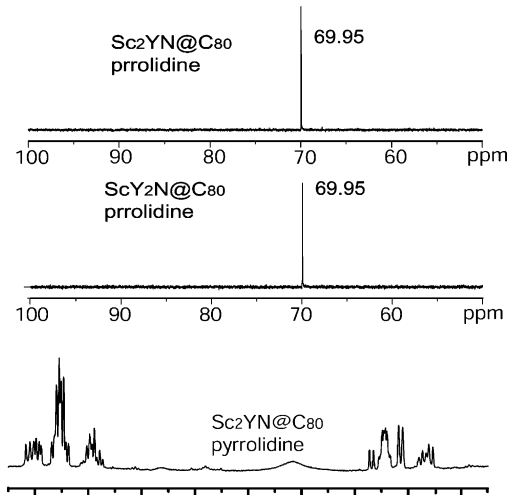

Figure 7. ^{13}C NMR spectra (150 MHz, top spectra) and ^1H NMR spectra (600 MHz, bottom spectra) of ^{13}C-enriched *N*-ethyl pyrrolidinofullerene derivatives of $Sc_2YN@C_{80}$ and $ScY_2N@C_{80}$.

TABLE 1: PBE/DNP-Predicted Key Geometric Parameters (Bond Length in Å, Angle in Degree) of $Sc_{3-x}Y_xN@C_{80}$ ($x = 0-3$) and Their Formation Energies (RE, in kcal/mol) and Energy Differences (ΔE, in kcal/mol) of the [6,6]- and [5,6]-Regioisomers of Pyrrolidinofullerenes

	$Sc_3N@C_{80}$	$Sc_2YN@C_{80}$	$ScY_2N@C_{80}$	$Y_3N@C_{80}$
Sc−N	2.03	1.98	1.93	
Y−N		2.14	2.10	2.05
Sc−C[a]	2.26	2.25	2.23	
Y−C[a]		2.39	2.37	2.36
		reaction energy		
[6,6]-adduct	−34.1	−35.6	−40.8	−44.3
[5,6]-adduct	−45.8	−45.5	−45.3	−44.8
ΔE[b]	11.7	9.9	4.5	0.5

[a] Nearest M to C(cage) distance. [b] $\Delta E = E_{tot}$(6,6-adduct) − E_{tot}(6,5-adduct).

The ^1H NMR spectra of them (Figure 7) agree well with such an assignment.

Therefore, our experiments clearly revealed that $Sc_3N@C_{80}$ and $Sc_2YN@C_{80}$ produce only the [5,6]-pyrrolidine regioisomers, and a critical change in fullerene regioselectivity occurs from $ScY_2N@C_{80}$ where the [6,6]-pyrrolidine regioisomer appears as a minor regioisomer and finally becomes the major regioisomer in the case of $Y_3N@C_{80}$. This result agrees well with the electronic property study of $Sc_{3-x}Y_xN@C_{80}$ ($x = 0-3$).

Finally, the size effect of M_3N acting on the metallofullerene property and reactivity was explored by means of density functional theory. The geometric structures of $Sc_{3-x}Y_xN@C_{80}$ ($x = 0-3$) were optimized at the PBE/DNP level of theory with the Dmol3 code.[25] As shown in Table 1, the M−N/M−C (M = Sc, Y) bond lengths decrease continuously from $Sc_3N@C_{80}$ to $Y_3N@C_{80}$, revealing that M_3N nuclei must bear increasing stresses along with the increase of the nuclear size. In the meantime, C_{80} must endure increasing stress and structural distortion due to the increasing size of the M_3N moiety. It is natural to imagine that the structural distortion of the fullerene cage would induce a substantial change of the fullerene's electronic property and reactivity.[20]

To examine the different reactivities of the four metallofullerenes $Sc_{3-x}Y_xN@C_{80}$ ($x = 0-3$), the formation energies of [5,6]- and [6,6]-pyrrolidino regioisomers were calculated. For simplicity, we adopted a simplified structural model, in which the $-C_2H_5$ group in the pyrrolidine part is replaced by a −H group.[26] As shown in Table 1, the calculated energies of the [5,6] regioisomers of $Sc_{3-x}Y_xN@C_{80}$ ($x = 0-3$) are always lower than that of the corresponding [6,6] regioisomers, indicating that the [5,6] regioisomers are thermodynamically more stable. This prediction is in line with the previous experimental observation that the addition to the [5,6] site of $M_3N@C_{80}$ (M = Sc, Y) is thermodynamically favored, but the addition to the [6,6] site is kinetically favored.[22a] However, the energy difference between the [6,6] and the [5,6] regioisomers decreases remarkably from 11.7 kcal/mol for the $Sc_3N@C_{80}$ case to only 0.5 kcal/mol for the $Y_3N@C_{80}$ case, with a sharp decrease (5.4 kcal/mol) observed between $Sc_2YN@C_{80}$ and $ScY_2N@C_{80}$ derivatives. Thus, according to the Hammond postulate,[27] the activation energy required for isomerization from the [6,6] regioisomer to the [5,6] regioisomer[22a] should increase with the increase of the size of the M_3N moiety, and thus, the isomerization becomes much more sluggish for the latter two endofullerenes, as was observed in our experiments.

Conclusion

Through comparative studies of $Sc_{3-x}Y_xN@C_{80}$ ($x = 0-3$), it is observed that $Sc_3N@C_{80}$ and $Sc_2YN@C_{80}$ have nearly the same electronic structures and frontier orbitals, and $ScY_2N@C_{80}$ and $Y_3N@C_{80}$ do as well. A critical transformation on the molecular frontier orbitals occurs at the point from $Sc_2YN@C_{80}$ to $ScY_2N@C_{80}$. The chemical reactivity of $Sc_{3-x}Y_xN@C_{80}$ ($x = 0-3$) is checked via the 1,3-dipolar cycloaddition reaction of *N*-enthylazomethine ylide, and the results confirm the critical change of regioselectivity between $Sc_2YN@C_{80}$ and $ScY_2N@C_{80}$. These findings show that the size of the endohedral moiety plays an important role in affecting the electronic properties and chemical properties of endohedral fullerenes, even though they have similar geometric structures.

Acknowledgment. The authors thank Professor Echegoyen and Dr. Cardona for in-depth discussions on the fullerene reactivity. C.R.W. thanks NSFC (Nos. 20573132, 90206045, and 20121301), the Major State Basic Research Program of China "Fundamental Investigation on Micro-Nano Sensors and Systems based on BNI Fusion" (Grant 2006CB300402). X.L. thanks NSFC (Nos. 20425312, 20673088, 20423002, 20021002, and 20203013).

Supporting Information Available: Details of the separation of $Sc_xY_{3-x}N@C_{80}$ ($x = 0-3$), Chromatograms and mass spectra of isolated $Sc_xY_{3-x}N@C_{80}$ ($x = 0-3$), detailed spectroscopic data of $Sc_xY_{3-x}N@C_{80}$ ($x = 0-3$), mass spectra of monoadduct of pyrrolidinofullerenes,. This information is available free of charge via the Internet at http://pubs.acs.org.

References and Notes

(1) Shinohara, H. *Rep. Prog. Phys.* **2000**, *63*, 843−892.

(2) (a) Klingeler, R.; Kann, G.; Wirth, I.; Eisebitt, S.; Bechthold, P. S.; Neeb, M.; Eberhardt, W. *J. Chem. Phys.* **2001**, *115*, 7215−7218. (b) Bolskar, R. D.; Benedetto, A. F.; Hudebo, L. O.; Price, R. E.; Jackson, E. F.; Wallace, S.; Wilson, L. J.; Alford, J. M. *J. Am. Chem. Soc.* **2003**, *125*, 5471−5478. (c) Krause, M.; Dunsch, L. *Angew. Chem. Int. Ed.* **2005**, *44*, 1557−1560. (d) Li, C. J.; Guo, Y. G.; Li, B. S.; Wang, C. R.; Wan, L. J.; Bai, C. L. *Adv. Mater.* **2005**, *17*, 71−73.

(3) Komatsu, K.; Murata, M.; Murata, Y. *Science* **2005**, *307*, 238−240.

(4) (a) Murphy, T.; Pawlik, T.; Weidinger, A.; Hohne, M.; Alcala, R.; Spaeth, J. M. *Phys. Rev. Lett.* **1996**, *77*, 1075−1078. (b) Kanai, M.; Porfyrakis, K.; Briggs, G. A.; Dennis, T. J. S. *Chem. Commun.* **2004**, 210−211.

(5) (a) Saunders, M.; Cross, R. J.; Jimenez-Vazquez, H. A.; Shimshi, R.; Khong, A. *Science* **1996**, *271*, 1693−1697. (b) Syamala, M. S.; Cross, R. J.; Saunders, M. *J. Am. Chem. Soc.* **2002**, *124*, 6216−6219.

(6) (a) Dennis, T. J. S.; Shinohara, H. *Chem. Commun.* **1998**, 883−884. (b) Xu, Z.; Nakane, T.; Shinohara, H. *J. Am. Chem. Soc.* **1996**, *118*, 309−310.

(7) Cao, B.; Suenaga, K.; Okazaki, T.; Shinohara, H. *J. Phys. Chem. B* **2002**, *106*, 9295−9298.

(8) (a) Lian, Y.; Yang, S. *J. Phys. Chem. B* **2002**, *106*, 3112−3117. (b) Weiden, N.; Kato, T.; Dinse, K. P. *J. Phys. Chem. B* **2004**, *108*, 9469−9474.

(9) (a) Wang, C. R.; Kai, T.; Tomiyama, T.; Yoshida, T.; Kobayashi, Y.; Nishibori, E.; Takata, M.; Sakata, M.; Shinohara, H. *Angew. Chem. Int. Ed.* **2001**, *40*, 397−399. (b) Shi, Z. Q.; Wu, X.; Wang, C. R.; Lu, X.; Shinohara, H. *Angew. Chem. Int. Ed.* **2006**, *45*, 2107−2111. (c) Tan, K.; Lu, X.; Wang, C.-R. *J. Phys. Chem. B* **2006**, *110*, 11098−11102. (d) Tan, K.; Lu, X. *J. Phys. Chem. A* **2006**, *110*, 1171−1176. (e) Tan, K.; Lu, X. *Chem. Commun.* **2005**, 4444−4446.

(10) (a) Stevenson, S.; Rice, G.; Glass, T.; Harich, K.; Cromer, F.; Jordan, M. R.; Craft, J.; Hadju, E.; Bible, R.; Olmstead, M. M.; Maitra, K.; Fisher, A. J.; Balch, A. L.; Dorn, H. C. *Nature* **1999**, *401*, 55−57. (b) Olmstead, M. H.; de Bettencourt-Dias, A.; Duchamp, J. C.; Stevenson, S.; Marciu, D.; Dorn, H. C.; Balch, A. L. *Angew. Chem. Int. Ed.* **2001**, *40*, 1223−1225. (c) Olmstead, M. M.; Lee, H. M.; Duchamp, J. C.; Stevenson, S.; Marciu, D.; Dorn, H. C.; Balch, A. L. *Angew. Chem. Int. Ed.* **2003**, *42*, 900−903.

(11) (a) Yamada, M.; Feng, L.; Wakahara, T.; Maeda, Y.; Lian, Y.; Kako, M.; Akasaka, T.; Kato, T.; Kobayashi, K.; Nagase, S. *J. Phys. Chem. B* **2005**, *109*, 6049−6051. (b) Akasaka, T.; Kato, T.; Kobayashi, K.; Nagase, S.; Yamamoto, K.; Funasaka, H.; Takahashi, T. *Nature* **1995**, *374*, 600−601. (c) Wakahara, T.; Kobayashi, J.; Yamada, M.; Maeda, Y.; Tsuchiya, T.; Okamura, M.; Akasaka, T.; Waelchli, M.; Kobayashi, K.; Nagase, S.; Kato, T.; Kako, M.; Yamamoto, K.; Kadish, K. M. *J. Am. Chem. Soc.* **2004**, *126*, 4883−4887. (d) Akasaka, T.; Okubo, S.; Kondo, M.; Maeda, Y.; Wakahara, T.; Kato, T.; Suzuki, T.; Yamamoto, K.; Kobayashi, K.; Nagase, S. *Chem. Phys. Lett.* **2000**, *319*, 153−156.

(12) Yang, F. S.; Kalbac, M.; Popov, A.; Dunsch, L. *Chem. Phys. Chem.* **2006**, *7*, 1990−1995.

(13) Liduka, Y.; Lkenaga, O.; Sakuraba, A.; Wakahara, T.; Tsuchiya, T.; Yamada, M.; Nakahodo, T.; Akasaka, T.; Kobayashi, J.; Maeda, Y.; Okamura, M.; Waelchli, M.; Kobayashi, K.; Kako, M.; Mizorogi, N.; Nagase, S. *J. Am. Chem. Soc.* **2005**, *127*, 9956−9957.

(14) (a) Cardona, C. M.; Kitaygorodskiy, A.; Echegoyen, L. *J. Am. Chem. Soc.* **2005**, *127*, 10448−10453. (b) Cai, T.; Slebodnick, C.; Xu, L.; Harich, K.; Glass, T. E.; Chancellor, C.; Fettinger, J. C.; Olmstead, M. M.; Balch, A. L.; Gibson, H. W.; Dorn, H. C. *J. Am. Chem. Soc.* **2006**, *128*, 6486−6492. (c) Iezzi, E. B.; Duchamp, J. C.; Harich, K.; Glass, T. E.; Lee, H. M.; Olmstead, M. M.; Balch, A. L.; Dorn, H. C. *J. Am. Chem. Soc.* **2002**, *124*, 524−525. (d) Lee, H. M.; Olmstead, M. M.; Iezzi, E.; Duchamp, J. C.; Dorn, H. C.; Balch, A. L. *J. Am. Chem. Soc.* **2002**, *124*, 3494−3495.

(15) Chen, N.; Zhang, E. R.; Tan, K.; Wang, C. R.; Lu, X. *Org. Lett.* **2007**, *9*, 2011−2013.

(16) Krause, M.; Kuzmany, H.; Georgi, P.; Dunsch, L.; Vietze, K.; Seifert, G. *J. Chem. Phys.* **2001**, *115*, 6596−6605.

(17) (a) Iezzi, E. B.; Duchamp, J. C.; Fletcher, K. R.; Glass, T. E.; Dorn, H. C. *Nano Lett.* **2002**, *2*, 1187−1190. (b) Feng, L.; Xu, J. X.; Shi, Z. J.; He, X. R.; Gu, Z. N. *Chem. J. Chin. Univ.* **2002**, *23*, 996−998. (c) Yang, S. F.; Dunsch, L. *Chem. Eur. J.* **2006**, *12*, 413−419. (d) Chen, N.; Wang, C. R. *J. Phys. Chem. B* **2006**, *110*, 13322−13325. (e) Krause, M.; Dunsch, L. *Angew. Chem. Int. Ed.* **2005**, *44*, 1557−1560. (f) Olmstead, M. M.; de Bettencourt-Dias, A.; Duchamp, J. C.; Stevenson, S.; Dorn, H. C.; Balch, A. L. *J. Am. Chem. Soc.* **2000**, *122*, 12220−1222.

(18) Dunsch, L.; Krause, M.; Noack, J.; Georgi, P. *J. Phys. Chem. Solids* **2004**, *65*, 309−315.

(19) Cardona, C. M.; Kitaygorodskiy, A.; Ortiz, A.; Herranz, M. A.; Echegoyen, L. *J. Org. Chem.* **2005**, *70*, 5092−5097.

(20) Campanera, J. M.; Bo, C.; Poblet, J. M. *J. Org. Chem.* **2006**, *71*, 46−54.

(21) Echegoyen, L.; Chancellor, C. J.; Cardona, C. M.; Elliot, B.; Rivera, J.; lmstead, M. M.; Balch, A. L. *Chem. Commun.* **2006**, 2653−2655.

(22) (a) Cardona, C. M.; Elliott, B.; Echegoyen, L. *J. Am. Chem. Soc.* **2006**, *128*, 6480−6485. (b) Rodriguez-Fortea, A.; Campanera, J. M.; Cardona, C. M.; Echegoyen, L.; Poblet, J. M. *Angew. Chem. Ind. Ed.* **2006**, *45*, 8176−8180.

(23) Martin, N.; Altable, M.; Filippone, S.; Martin-Domenech, A.; Echegoyen, L.; Cardona. C. M. *Angew. Chem. Ind. Ed.* **2006**, *45*, 110−114.

(24) Martin, N. *Chem. Commun.* **2006**, 2093−2104.

(25) For the PBE density functional theory, see: (a) Perdew, J. P.; Burke, K.; Ernzerhof, M. *Phys. Rev. Lett.* **1996**, *77*, 3865. DNP refers to double numerical basis sets plus polarization. The Dmol^3 code was implemented in Material Studio, Accelrys Inc.; see: (b) Delley, B. *J. Chem. Phys.* **1990**, *92*, 508−517; (c) Delley, B. *J. Chem. Phys.* **2000**, *113*, 7756−7764.

(26) Considering the $-C_2H_5$ group is far from the pyrrolidine/fullerene bonding sites, this simplification should not affect the calculated reacting energies.

(27) Hammond, G. S. *J. Am. Chem. Soc*. **1954**, *77*, 334−338.